

Insights on the historical and emerging global land cover changes: The case of ESA-CCI-LC datasets



Alijafar Mousivand^{a,*}, Jamal Jokar Arsanjani^b

^a Remote Sensing and GIS Department, Tarbiat Modares University, Jalal AleAhmad, Nasr Bridge, PO Box 14115-111, Tehran, Iran

^b Geoinformatics Research Group, Department of Planning, Aalborg University Copenhagen, A.C. Meyers Vænge 15, DK-2450 Copenhagen, Denmark

ARTICLE INFO

Keywords:

ESA-CCI

Historical land change

Global land cover

Climate change

Predictive analytics

ABSTRACT

Global land cover (LC) mapping has been the main source of monitoring our global landscapes for a wide range of applications e.g., food production estimation, urbanization, deforestation, climate change studies, air/soil/water pollution, and CO₂ emission. Several initiatives and organizations have attempted to generate global LC maps using remote sensing data and in-situ data. Noteworthy examples include IGBP-DISCover, GlobeCover 2009, FAO, GLC 2000, MODIS, GlobeLand30. While researchers including climate change scientists require fine LC maps in terms of spatial resolution and temporal coverage for continuous monitoring of the planet, these datasets lack of fulfilling this goal. Understanding the trend of LC changes as well as the direction of future changes at global level is of vital importance to a broad spectrum of stakeholders, and essential for addressing the sustainable development goals worldwide. European Space Agency has recently released its climate change initiative's LC dataset called CCI-LC, which aims at achieving this ambition with 300 m spatial resolution and 24-year continuous temporal coverage within 1992–2015. The main objective of this study is to quantify the global land changes within this timeframe and also to predict the future land change by 2050 in order to gain a global picture of our future planet. This is a timely objective since more than ever scientists, environmentalist, and governors require to know how our future will look like and how they can achieve the goals of the United Nations Framework Convention on Climate Change (UNFCCC) i.e., the Paris Agreement. The achieved results reveal massive land changes of different kinds e.g., deforestation, urbanization, desertification, forestry, water and ice shrinkage across different continents. The employed predictive modelling for year 2030 and 2050 messages dramatic changes among different LC types. Our discussions and conclusive comments can guide policy-makers, environmental planners, ecosystem services providers and climate change researchers to gain finer insights about our planet by 2050. Future research direction draws attention for investigating the underlying causes and consequences on our ecosystems and human population.

1. Introduction

1.1. Land change science

Land change science (LCS), as an emerging interdisciplinary field, plays a key role in studying global environmental change and sustainability analysis. The primary focus of LCS is to pay more attention to understanding LC and land use (LU) dynamics as a human–environment process across space and time (Rindfuss, Walsh, Turner, Fox, & Mishra, 2004; Turner, Lambin, & Reenberg, 2007). Furthermore, LCS attempts to draw theories and concepts for explaining the underlying processes as well as proposing models for modelling these processes in order to address societal and environmental challenges arisen from them (Foley et al., 2005; Janetos et al., 2005; Turner et al., 2007). Hence, LCS

includes monitoring and observation of land resources, investigating the motivating causes, potential impacts, and foreseen consequences, modelling spatial-temporal land changes both in the past and the future, and drawing land policies and informing stakeholders (Ellis & Ramankutty, 2008; Verburg, Eck, Nijs, Dijst, & Schot, 2004).

Changes in LC/LU might have positive and negative impacts in our ecosystems at local, regional, and global scales (Symeonakis, 2016; Verburg, Neumann, & Nol, 2011). The major types of LC change appear in forms of urbanization (Jokar Arsanjani, Helbich, & Vaz, 2013; Nunes, Loures, Lopez-Piñero, Loures, & Vaz, 2016), deforestation and afforestation (Pineda Jaimes, Bosque Sendra, Gómez Delgado, & Franco Plata, 2010; Seto, Güneralp, & Hutrya, 2012), shrinkage and drying of wetlands and water resources (T. Jokar Arsanjani, Javidan, Nazemosadat, Jokar Arsanjani, & Vaz, 2015; Roach, Griffith, & Verbyla,

* Corresponding author.

E-mail address: a.mousivand@modares.ac.ir (A. Mousivand).

<https://doi.org/10.1016/j.apgeog.2019.03.010>

Received 9 December 2018; Received in revised form 16 February 2019; Accepted 23 March 2019

Available online 29 March 2019

0143-6228/ © 2019 Elsevier Ltd. All rights reserved.

2013), desertification (Higginbottom & Symeonakis, 2014; Sternberg, Tsolmon, Middleton, & Thomas, 2011). Some types of LCC have incorporated to our recent global concerns with respect to climate change, environmental quality, biodiversity loss, and water/air/soil pollution (Janssen, Dumont, Fierens, & Mensink, 2008; Zhang et al., 2016). LC dynamics have contributed to about 20% of global CO₂ emissions (Feddema et al., 2005; Mahmood, Pielke, & McAlpine, 2015), therefore, it is of outmost importance to have a continuous observation of LC and model the historical changes in order to have a big picture of the future dynamics. This has been flagged as a foremost importance for international and regional organizations, academia, policy makers, and involved stakeholders across the world to pay more attention to (Plummer, Lecomte, & Doherty, 2017).

1.2. Global LC products

Global LC maps are essential layers of information for a wide range of applications e.g., environmental monitoring, ecosystem services, environment quality analysis, climate change studies, among others (Fuchs, Prestele, & Verburg, 2018; Li et al., 2018). Furthermore, they have been the main source for our estimation of the exchange of energy and carbon between the Earth and the atmosphere, food production, hydrological processes, energy consumption, to name a few (Li et al., 2016; Rindfuss et al., 2004). Hence, a large number of remote sensing projects have been launched in order to generate regional and global LC maps at reasonable spatial, temporal, and thematic accuracy so that we can screen the historical change of our natural and anthropocentric resources while being able to predict the future (Arsanjani, 2018; Seto et al., 2012).

There are currently several regional and global LC products available, mainly based on remotely sensed data. These products are provided in different spatial and temporal resolutions and differ in many aspects e.g. classification scheme, LC types, accuracy, temporal domain. While global LC products are typically derived from coarse spatial resolution data such as AVHRR, MODIS, MERIS, and SPOT VEGETATION (e.g. IGBP-DISCover, MODIS Collection 4 and 5 Land Cover product, Glob-Cover) (Wulder et al., 2008), regional and national maps are often based on medium to high resolution satellite data (e.g. CORINE Land Cover 1990, 2000, 2006, and 2012 in Europe from Landsat, IRS, RapidEye and EOSD 2000 and 2007 in Canada derived from Landsat data, NLCD 2001, 2006, 2011, 2016 in the US derived from multiple dates of Landsat satellite imagery; Australian NCAS-LCCP). A detailed cross comparison of the existing global LC datasets is outlined in (Grekousis, Mountrakis, & Kavouras, 2015).

Several studies including (Deus & Gloaguen, 2013; Foley et al., 2005; Lambin et al., 2001; Rindfuss et al., 2004) have investigated the pattern, extent, and intensity of land changes across different continents and have reported massive LC changes within the recorded remote sensing observations. Different datasets have been used for this purpose, for instance, GlobCover 2009 (Arino et al., 2012), MODIS (Friedl et al., 2002), IGBP DISCover (Loveland et al., 2000), UMD Land Cover (Hansen, DeFries, Townshend, & Sohlberg, 2000), Global Land Cover 2000 (Bartholomé & Belward, 2005), and ESA-CCI-LC (Liu, Yu, Li, et al., 2018; Liu, Yu, Si, et al., 2018; Plummer et al., 2017). The latter is of high importance, since it offers a comparatively finer spatial resolution of 300 m as opposed to 1000 m for most of the others as well as a higher temporal resolution ranging from 1992 to 2015 with one-year intervals as detailed in Section 2.1.

1.3. Land change models

In order to achieve the sustainable development goals, an estimated picture of the future planet is required so that we can take preparedness measures avoiding the destructive changes jeopardizing the planet, its inhabitants, and adequacy of the future supply while supporting the positive ecosystem changes. For doing so, a set of land change models

have been developed and proposed. The most popular and frequently-used models are Cellular Automata (CA) (Clarke & Gaydos, 1998; Jamal JOKAR Arsanjani, Fibæk, & Vaz, 2018), Markov chain (Alimohammadi, Mousivand, & Shayan, 2010), CA-Markov (Yang, Zheng, & Chen, 2014), logistic regression (Dubovyk, Sliuzas, & Flacke, 2011), agent-based model (Haase, Lautenbach, & Seppelt, 2010; Jamal JOKAR Arsanjani et al., 2013) and CLUE (Verburg & Overmars, 2009), LTM (Tayyebi & Pijanowski, 2014). These models greatly differ in terms of their underlying rationale, user input e.g., neighbourhood effect, form of temporal transition, as well as socio-economic factors being reflected in the model. Thus, they result in dissimilar outputs, sometimes close to reality or contradictory. For an extensive literature review on the existing models, their principles, and their application in different case studies, please see (Aburas et al., 2016).

In this study, Markov chain model was chosen. The reasons for choosing Markov chain model include: a) the ability to quantify changes across land types i.e., the size of changes, b) the form of change i.e., change from forest to built-up, c) acquiring the probability of change across land types e.g., it is 86% probable that a forest pixel will be converted to a farm pixel, d) finally, the possibility of running it over large multi-temporal datasets. The latter was a decisive criterion for this study, because most tools implementing these models struggle handling large size datasets e.g., ESA-CCI. As an advantage of Markov chain, large-size datasets can be imported in the model.

The main objective of this study is to characterize the past global LC patterns and the changes within a 24-year timeframe. Furthermore, it aims at predicting the upcoming LC changes using the historical changes and a Markov chain model.

Hence, the following research questions are intended to be addressed in this paper:

- What is the typology of land change across the planet according to ESA-CCI datasets?
- What is the magnitude of change across different continents? And what are their implications?
- How will the future patterns of land change e.g., by 2030 and 2050 look like using predictive approaches and historical trends?

The remainder of this paper is structured as follows. Section 2 describes the data and materials used in the study and Section 3 presents the utilized methods. Section 4 presents the results, while Section 5 discusses our findings. Finally, the conclusions are drawn in Section 6.

2. Materials

2.1. Data and study area

European Space Agency (ESA) launched their Climate Change Initiative (CCI) programme aiming at providing high quality satellite-derived products of Essential Climate Variables (ECVs), including LC, as suggested by the Global Climate Observing System, e.g., Bojinski et al. (2014). The main objective of the project was to provide a consistent historical LC dataset for climate modelling purposes. The ESA-CCI-LC dataset presents a consistent multi-temporal global LC maps at 300 m spatial resolution covering 1992 to 2015 with one-year intervals. This product is developed using the GlobCover unsupervised classification chain and merging multiple available earth observation products based on ESA's GlobCover products. Unlike many remote sensing products that are based on single-year and single-sensor approaches, this dataset is generated using multiple sensors e.g., Advanced Very High Resolution Radiometer (AVHRR) Systeme Probatoire d'Observation de la Terre Vegetation (SPOT-VGT), and PROBA-V with a reported overall weighted-area accuracy of about 71% (Defourny et al., 2008). A total of 37 original LC types are presented using the LC Classification System developed by the FAO (Defourny, Moreau, & Bontemps, 2017). Interested readers are referred to (Plummer et al., 2017) for more details. In

Table 1

A look up table for reclassification of land cover types (adapted from Land Cover CCI: product user guide, Version 2, available at https://www.esa-landcover-cci.org/?q=webfm_send/84).

Classes considered in this study	Land types used in the CCI-LC maps	
1. Agriculture	10, 11, 12 20 30 40	Rainfed cropland Irrigated cropland Mosaic cropland (> 50%)/natural vegetation (tree, shrub, herbaceous cover) (< 50%) Mosaic natural vegetation (tree, shrub, herbaceous cover) (> 50%)/cropland (< 50%)
2. Forest	50 60, 61, 62 70, 71, 72 80, 81, 82 90 100 160 170	Tree cover, broadleaved, evergreen, closed to open (> 15%) Tree cover, broadleaved, deciduous, closed to open (> 15%) Tree cover, needleleaved, evergreen, closed to open (> 15%) Tree cover, needleleaved, deciduous, closed to open (> 15%) Tree cover, mixed leaf type (broadleaved and needleleaved) Mosaic tree and shrub (> 50%)/herbaceous cover (< 50%) Tree cover, flooded, fresh or brakish water Tree cover, flooded, saline water
3. Grassland	110 130	Mosaic herbaceous cover (> 50%)/tree and shrub (< 50%) Grassland
4. Wetland	180	Shrub or herbaceous cover, flooded, fresh-saline or brakish water
5. Settlement	190	Urban
6. Sparse vegetation	120, 121, 122 140 150, 151, 152, 153	Shrubland Lichens and mosses Sparse vegetation (tree, shrub, herbaceous cover)
7. Bare area	200, 201, 202	Bare areas
8. Water	210	Water
9. Permanent snow and ice	220	Permanent snow and ice

this study, the global coverage and the entire ESA-CCI-LC dataset ranging from 1992 to 2015 is used.

2.2. Reclassification of ESA-CCI LC nomenclature

For this study, the original 37 LC classes were reclassified into 9 major LC types: agriculture, forest, grassland, bare area, wetland, open water, settlement, sparse vegetation and permanent ice/snow cover. The original and adapted classes are presented in Table 1.

Fig. 1, as an example, shows ESA-CCI LC dataset for 2015 using the

look up table presented above.

3. Methods

In order to determine the extent of LC change, pixel count multiplied by pixel area method is used for calculating temporal changes. Thereafter, a Markov chain model (as in *Jokar Arsanjani, Kainz, and Mousivand (2011); Alimohammadi Mousivand & Shayan (2010)*) was used to generate transition area matrices as well as transition probabilities matrices. Transition area matrix presents the predicted areal

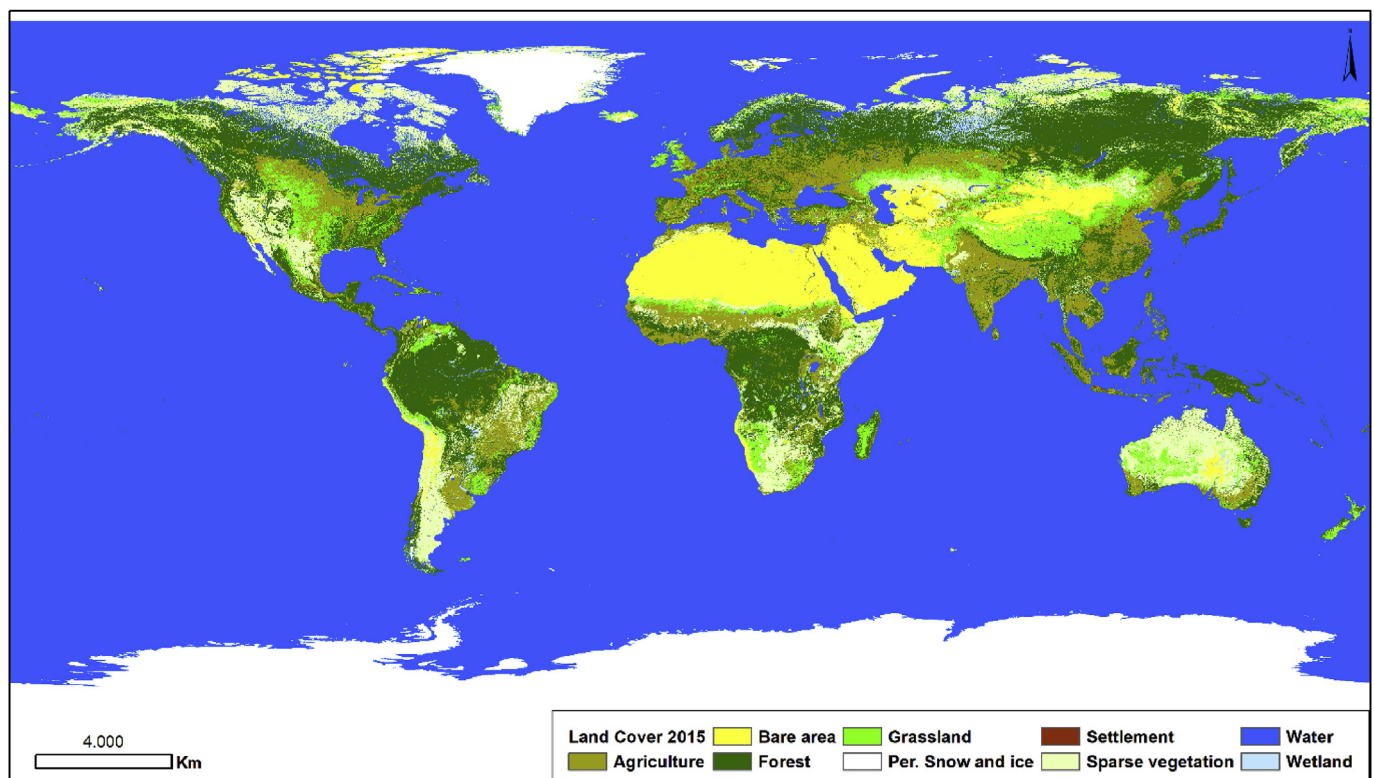


Fig. 1. The LC map of year 2015 at 300 m spatial resolution.

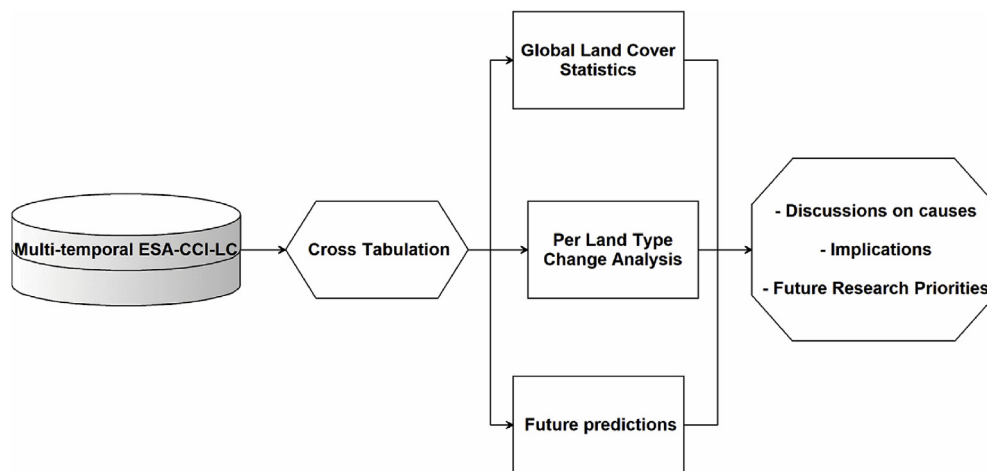


Fig. 2. A schematic flowchart of the study.

change from each class to another, while transition probabilities matrix gives the probability values for each class to be converted to another class. The generated transition area matrix is useful for identifying systematic LC transitions as outlined by [Alo & Robert Gilmore Pontius \(2008\)](#). Fig. 2 illustrates the schematic flowchart of the study.

4. Results

4.1. Historical changes

From the viewpoint of the historical changes among the nine LC types, we employed three different criteria to quantify the amount of change and conversion rate among different classes. These criteria include (i) historical change trend; (ii) gain and loss figures; and (iii) transition area matrices per LC class from 1992 to 2015. In order to have equally time-sampled transition matrices of 10-year, we decided to consider the transition matrices of two equivalent timeframes; one from 1995 to 2005 and another one from 2005 to 2015.

Fig. 3 shows per-class statistics of the historical changes in the area of nine distinct LC types over the period of 24 years. It should be noted that due to the substantial area variability among LC types, different data scales were used for y-axis avoiding loss of small variations. Fig. 4 presents the values of gain and loss per LC type calculated in terms of area, change percentage and area percentage between 1992 and 2015. Transition matrices of two distinct 10-year time periods are shown in Fig. 5, in which different colours represents the conversion rate among LC types. Finally, Fig. 6 illustrates the spatial distribution of change/conversion among different LC type across the globe over the entire time period.

As shown in Fig. 3, on the one hand, five LC types including forest, wetland, bare land, shrubland/sparse vegetation and water showed a decreasing trend with small oscillation in different spans likely due to unsteady changes globally from year to year. On the other hand, agriculture, settlement and grassland areas increased over time with settlement showing most marked increase by 60%. Fig. 4 illustrates that the most gain is observed in the settlement class and the most loss occurred in the wetland area up to 15%. From the maps in Fig. 5, it is evident that the Amazonian deforestation is the major contributors to the loss of forest cover globally, and the conversions from water to other classes mainly emerged in the form of disappearing lakes in parts of Asia. The results of the LC conversion analysis given in Fig. 6, also indicates that the settlement and permanent snow and ice classes were persistent over time, whereas forest and agriculture experienced dramatic conversion to other LC types. We will discuss the historical changes of each class in further detail in terms of the three above-mentioned criteria.

4.1.1. Agriculture

A closer look at the graphs indicates that agriculture has a clear ascending tendency from 1994 to 2004 with an increase of 0.8 million sqkm and then continues with a less steep progression until 2015. In total, agriculture increased from 29.019 to 29.864 million sqkm globally over these years. Further analysis showed that approximately 2.2 million sqkm lands turned into agriculture lands, while about 1.3 million sqkm agriculture lands disappeared and been replaced by other LC types (see Fig. 4). In terms of areal percentage, land under agriculture was growing by 7.07 percent and concurrently declining by 4.37 percent in different regions, resulting in 2.7 percent net increase in total between 1992 and 2015. From Fig. 5, it is interesting to see that most spatial changes in agricultural land between 1992 and 2015 occurred in central and Eastern Europe, Central African countries, South America and China. The observed changes in agriculture are perceived as due to conversion between agriculture and forest, as well as agriculture and settlement within this period (Fig. 6).

Fig. 6 shows that agricultural lands were converted by 0.24 and 0.09 to forest and settlement, respectively (1995–2005). On the other hand, forest by 0.28 and shrubland/sparse vegetation by 0.16 and grassland by 0.12 were converted to agriculture. From 2005 to 2015, conversion from agriculture to forest dropped to 0.18, while conversion from agriculture to settlement slightly increased to 0.10. Similarly, forest conversion to agriculture is about 0.14% and both shrubland/sparse vegetation and grassland converted to agriculture by about 0.07. The persistence of agriculture increased from about 0.61 in the time period of 1995–2005 to 0.68 in 2005–2015.

4.1.2. Forest

As depicted in Fig. 3, forest LC shows a decreasing trend with an overall decrease of about 0.357 million sqkm over the same time period. However, what stands out in this figure is the increase in forest from 1999 till 2007 with a value of about 0.219 million sqkm. The results, in terms of forest cover gain and loss percentage, in Fig. 4 also illustrates that a gain of 3.85 percent and a loss of 4.44 percent was seen in the forest cover, resulting in a net decrease of 0.059 percent. The spatial maps in Fig. 5 depict that significant deforestation has obviously occurred in Amazon and Central-East Africa within 24 years. Moreover, Indonesia and eastern China have also experienced dramatic declines in the forest cover over the time period. Fig. 6 illustrates the direction of these changes from/to forest cover. The major classes converted to forest are agriculture, wetland and shrubland/sparse vegetation with 0.24, 0.23 and 0.21 (1995–2005) and, with 0.18, 0.15 and 0.16 (2005–2015) transition probabilities, respectively. Likewise, forest cover was converted to agriculture, shrubland/sparse vegetation and grassland with 0.28, 0.14 and 0.07 (1995–2005) and, with 0.14, 0.16

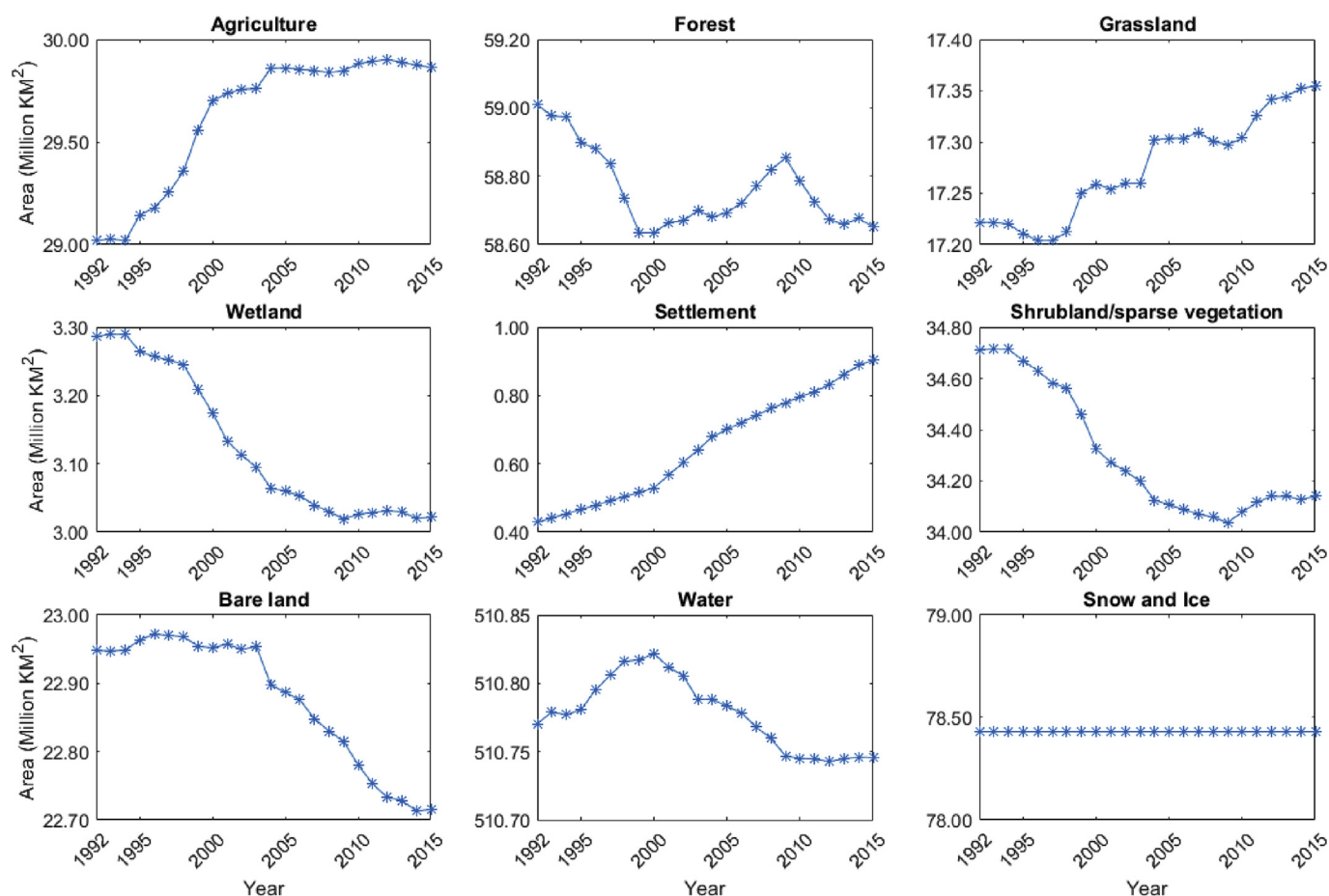


Fig. 3. Global historical changes in the area of nine distinct LC types from 1992 to 2015.

and 0.05 (2005–2015) transition probabilities, respectively. The persistence probability for forest cover was 0.43 for the 1995–2005 and 0.59 for the 2005–2015 time periods, presenting the least stability among all LC types.

4.1.3. Grassland

Grassland area, as seen in Fig. 3, increased over time, although some fluctuations are present for some years. The area of grassland expanded from 17.221 to 17.354 million sqkm over the time period, translating to a net growth of 0.133 million sqkm. Additionally, the gain in grassland

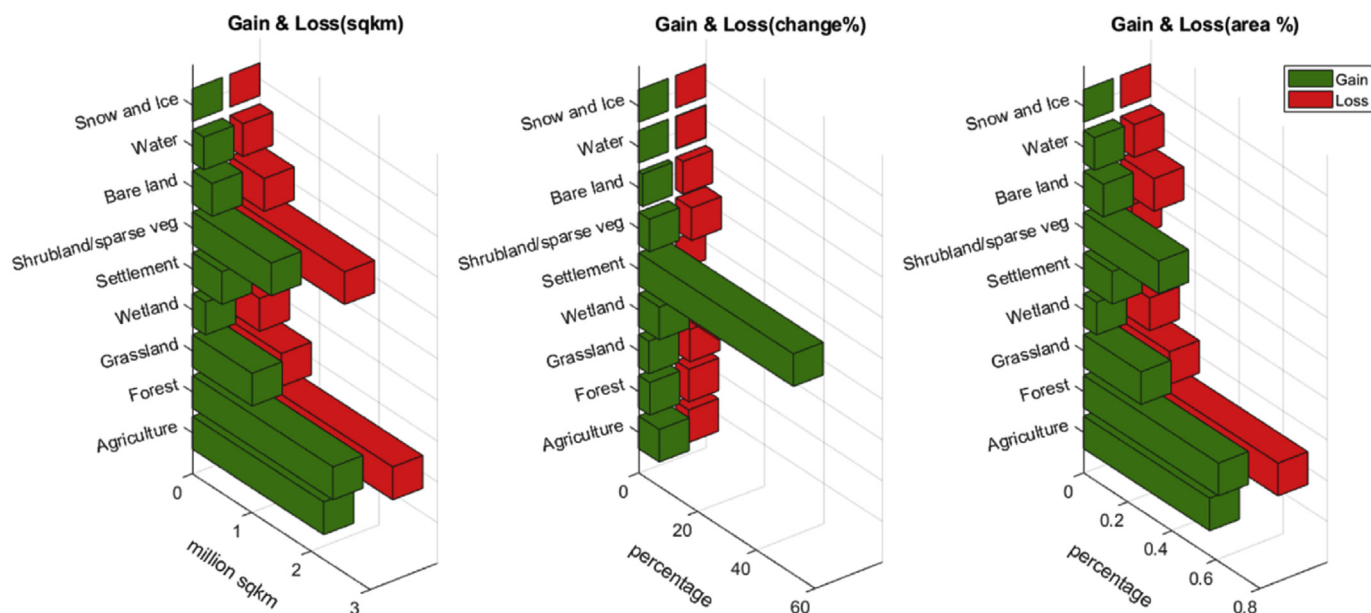


Fig. 4. Gain and losses in all land cover types between 1992 and 2015. % change: (pixels changes for a class/area of a class in the later land cover image) *100, and % of area: (pixels changes for a class/total area of the land cover map) *100.

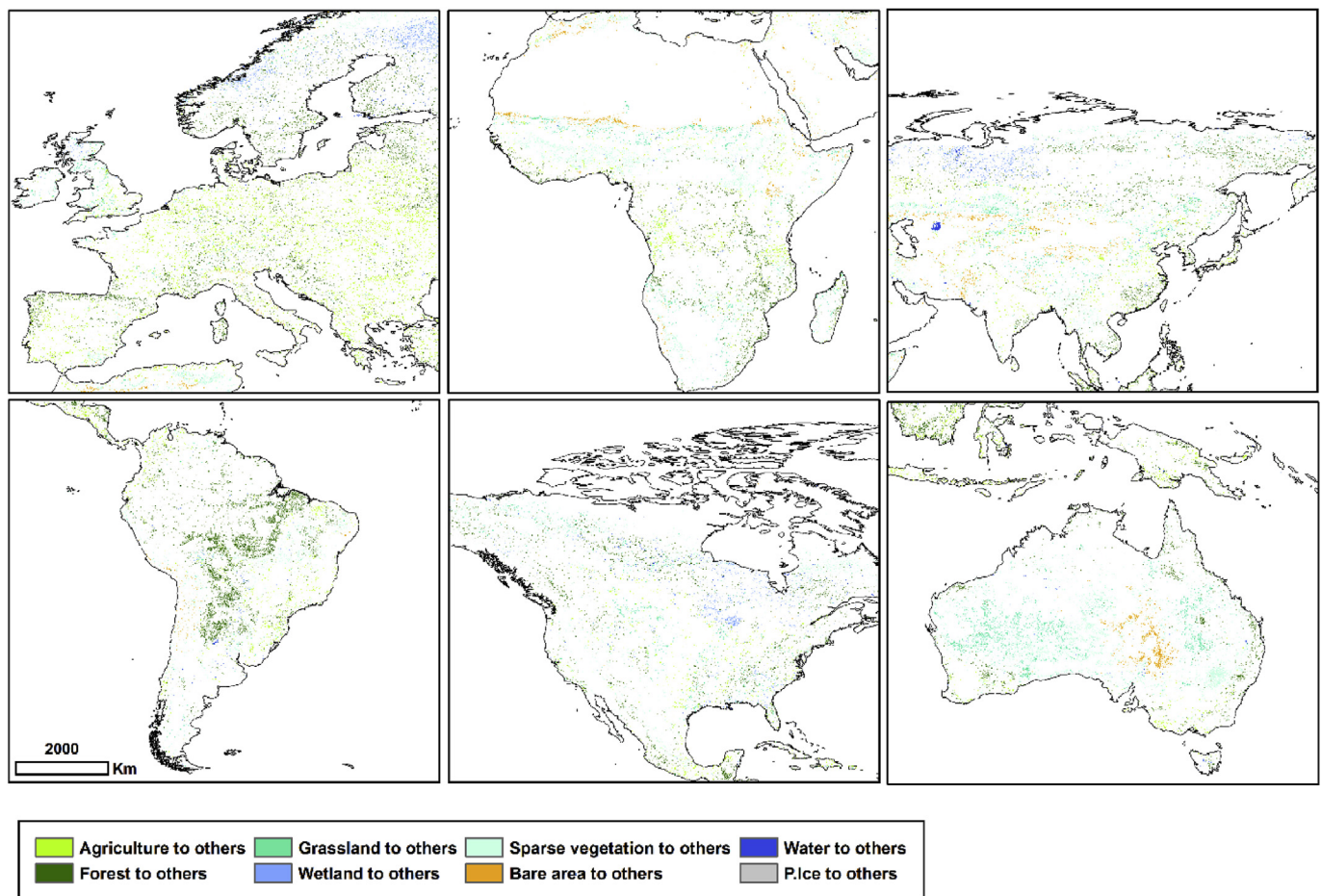


Fig. 5. Land change maps and their types across continents.

was around 3.52%, while a loss of 4.80% occurred in the same time (Fig. 4). The most increase is seen between 2003 and 2004, and most loss is also between 2007 and 2008. Fig. 6 shows that major conversions occurred from grassland to agriculture (0.11), forest (0.08) and shrubland/sparse vegetation (0.08), while conversion from other classes to grassland is in forest (0.07), shrubland/sparse vegetation (0.08) and bare land (0.11) between 1995 and 2005. Likewise,

conversions from grassland to agriculture (0.07), forest (0.07) and shrubland/sparse vegetation (0.07) and from forest (0.05), shrubland/sparse vegetation (0.08) and bare land (0.06) to grassland are characterized as the dominant conversions occurred between 2005 and 2015. The consistency of grassland increased from 0.67 to 0.76 between the two time periods.

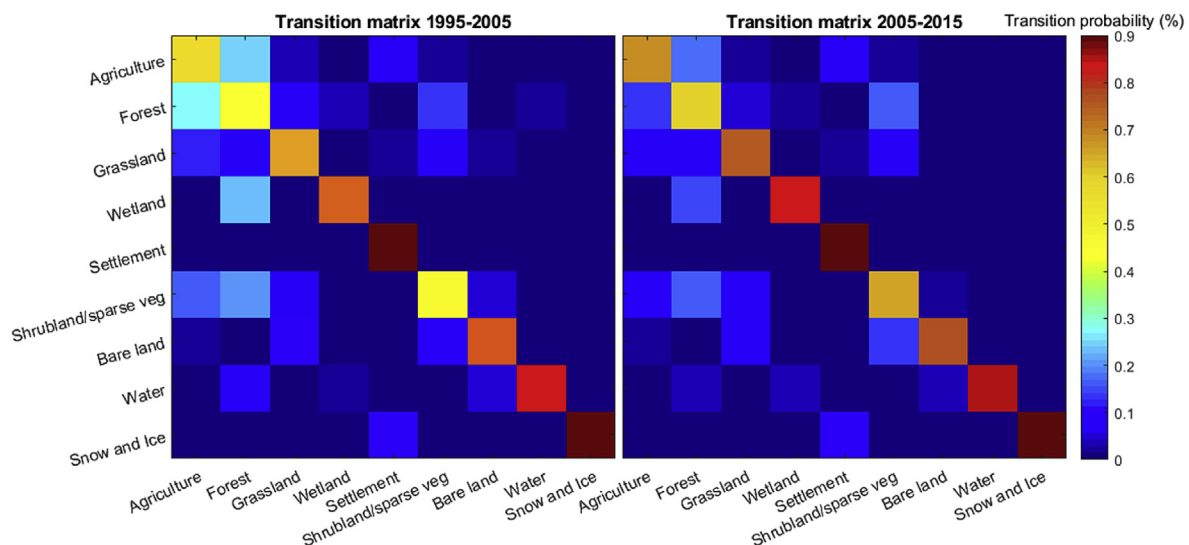


Fig. 6. Transition matrices of different land cover types from 1995 to 2005 and from 2005 to 2015.

4.1.4. Wetland

Fig. 3 reveals that there was a dramatic fall in the area of wetlands from 1992 to 2009, however, it slowed down since 2009 becoming more stable. A total decrease of 0.264 million sqkm was recorded over 24 years in the wetland areas globally. Fig. 4 shows that the percentage loss was more than twice the percentage gain, with values of 14.53% versus 7.06% for loss and gain, respectively. These changes are mainly due to a rather remarkable conversion from wetland to forest about 0.23 (1995–2005) and 0.15 (2005–2015), whereas other conversions are marginal with the maximum value of about 0.009 for conversion from wetland to water (Fig. 5). Furthermore, major conversions were from forest to wetland (0.04), and water to wetland (0.02) (1995–2005) and from forest to wetland (0.03), and water to wetland (0.04) (2005–2015). Wetland areas became more stable in the second time period (2005–2015) that the first (1995–2005) rising up stability from 0.74 to 0.84.

4.1.5. Settlement

Settlement proved to be the most varying LC type all over the world with an areal increase of 52.48% since 1992. From Fig. 3 it is seen that settlement substantially increased from 0.429 up to 0.904 million sqkm. It comes with no surprise that the loss of settlement is zero over the time period, while the gain doubled (Fig. 4). The interesting part, however, is about the conversion from other LC types to settlement over time, in which settlement encroached about 0.09 of agriculture, 0.02 of grassland and 0.10 of permanent ice and snow cover over both time periods with a little increase in 2005–2015. Although it is unlikely to change from settlement to other classes in reality, the results indicate that almost 0.01 of the area of settlement (Fig. 6) were converted to other LC types for both time periods. The probability of settlement to persist over both time periods is 0.9, making it the most stable class among all.

4.1.6. Shrubland/sparse vegetation

In Fig. 3, there is a clear trend of decreasing for shrubland/sparse vegetation pretty similar to the one from wetlands over time. This LC type decreased from 34.713 in 1992 to 34.140 million sqkm, with a net decrease of 0.572 million sqkm. The gain was 3.72% versus a loss of 5.31% in the percentage of shrubland/sparse vegetation from 1992 to 2015.

It is inferred from Fig. 5 that considerable conversion occurred in Australia, African countries along the Sahara Desert, USA and Asian countries (in particular China and Kazakhstan). Over the time period of 1995–2005, shrubland/sparse vegetation was mainly converted to agriculture (0.16), forest (0.21), grass (0.08) and bare land (0.05). A decrease was seen in the conversion of shrubland/sparse vegetation to other class type in 2005–2015 with conversion to agriculture (0.07), forest (0.15), grass (0.08) and bare land (0.02). The conversion rate from other LC types to shrubland/sparse vegetation were 0.13 for forest, 0.08 for grassland and 0.09 for bare land in 1995–2005 and 0.16 for forest, 0.07 for grassland and 0.13 for bare land in 2005–2015 (Fig. 6). The stability of this LC type increased from 0.49 (1995–2005) to 0.66 (2005–2015), although still being the second most unstable class.

4.1.7. Bare land

Bare land area decreased from 22.948 in 1992 to 22.715 million sqkm in 2015 with a net decrease of about 0.232. The pattern, as shown in Fig. 3, fell over time with an exception for a short period between 1995 and 1999 showing small increasing variation. From Fig. 4, bare land gained 1.40% versus a loss of 2.40% over the time period. Fig. 5 shows the spatial distribution of bare land conversion to other LC types, where remarkable conversion took place in countries bordering the Sahara Desert, Asian countries (Iran, Kazakhstan, China and Pakistan) and Australia. Three major LC types with most conversion to bare land are grassland (0.03), shrubland/sparse vegetation (0.04) and water

(0.05) in 1995–2005 and grassland (0.01), shrubland/sparse vegetation (0.02) and water (0.04) in 2005–2015 (Fig. 6). On the other hand, bare land was mostly converted to agriculture (0.03), grassland (0.11), shrubland/sparse vegetation (0.09) in 1995–2005, and agriculture (0.02), grassland (0.06), shrubland/sparse vegetation (0.14) in 2005–2015. The class type stability increased from 0.75 in 1995–2005 to 0.77 in 2005–2015.

4.1.8. Water

Water is by far the greatest LC type with an area of about 510.770 sqkm in 1992 corresponding to 67.58% of the planet decreasing to 510.745 million sqkm in 2015 (67.57%), resulting in a net decline of 0.025 million sqkm. There was no gain for water bodies, however, a loss of 0.17% occurred over the time period. Spatial distribution of changes in water (mainly inland water bodies) in Fig. 5 highlights disappearing lakes in Asia (e.g. Aral Sea and Urmia Lake), as well as reducing water body areas worldwide. Water bodies were mainly converted to forest (0.06), wetland (0.02) and bare land (0.05) in 1995–2005 and to forest (0.04), wetland (0.04) and bare land (0.04) in 2005–2015 (Fig. 6). The major LC types that were converted to water are forest (0.02) and settlement (0.01) in 1995–2005 and forest (0.01) and settlement (0.01) in 2005–2015. The stability of water bodies slightly increased over time from 0.83 in 1995–2005 to 0.85 in 2005–2015.

4.1.9. Permanent ice and snow

Permanent ice and snow cover shows quite steady pattern over time with only a marginal drop in 2014. Overall, no gain or loss is evident for this land type and was only converted to settlement (0.10) in both time frames. Settlement is the only cover type being converted to ice and snow by 0.01. Permanent ice and snow cover type was persistence over time with 0.90 stability.

4.2. Markov chain predictions

After historical change analysis, a Markov chain analysis was conducted to predict the upcoming changes in the future. The Markov chain model is a stochastic modelling approach that results in probability surfaces of land change from land type A to B. The model has been extensively used in LC/LU change modelling (Vaz & Arsanjani, 2015). The model concludes the size of area subject to conversion from A to B along with the probability values for change. (Zhou et al., 2012; Kamusoko et al., 2009). As a result, the transition areas' matrices of change within 2015–2030 and 2015–2050 have been generated in the following.

Tables 2 and 3 provide transition area matrices in terms of area (million sqkm) and probability (%) from 2015 to 2030 and 2015–2050. These tables highlight interesting statistics on the conversion rates among different LC types in future. According to Markov predictions, agriculture consistency will drop to 55.6% and 39% in 2030 and 2050, respectively. The results show that agriculture will mostly convert to forest (31.4% in 2030 and 29.8% in 2050) and settlement (9.9% in 2030 and 16.7% in 2050). Surprisingly, the rate of conversion from agriculture to settlement (2030) will be about 2.2 million ha per month, which is equivalent to 28 times the area of New York.

Forest cover is the most vulnerable class and expected to experience severe decline as only 37.2% and 26.2% of its cover will remain in 2030 and 2050, respectively. Agriculture (30.4% in 2030 and 32.9% in 2050) and shrubland/sparse vegetation (19.1% in 2030 and 17.4% in 2050) are the two main classes to which forest cover converts. 66.4% (2030) and 46.4% (2050) of grassland will remain unchanged, while 11.1%, 9.6% and 8.6% (2030) and 17.5%, 12.7% and 14.3% (2050) of them will convert to agriculture, shrubland/sparse vegetation and forest, respectively. Predictions indicate that wetland area consistency will drop to 74.7% and 59.4% in 2030 and 2050 with most conversion to forest by 24.5% (2030) and 28.6% (2050). 72.9% of bare land area will remain in 2030, while 14.3% and 9.8% will convert to shrubland/

Table 2

The transition area matrix presenting the expected land change from the horizontal classes to the vertical classes in terms of million sqkm and percentage (2015–2030).

	Agriculture	Forest	Grassland	Wetland	Settlement	Sparse vegetation	Bare area	Water	P. snow and Ice
Agriculture	22.37	12.65	0.98	0.00	3.99	0.00	0.13	0.12	0.00
	55.6	31.4	2.4	0.0	9.9	0.0	0.3	0.3	0.0
Forest	12.74	15.57	2.80	1.64	0.00	7.99	0.15	1.00	0.00
	30.4	37.2	6.7	3.9	0.0	19.1	0.4	2.4	0.0
Grassland	3.03	2.37	18.21	0.00	0.42	2.63	0.70	0.08	0.00
	11.1	8.6	66.4	0.0	1.5	9.6	2.6	0.3	0.0
Wetland	0.00	4.69	0.00	14.31	0.05	0.00	0.00	0.10	0.00
	0.0	24.5	0.0	74.7	0.3	0.0	0.0	0.5	0.0
Settlement	0.13	0.13	0.13	0.13	9.04	0.13	0.13	0.13	0.13
	1.3	1.3	1.3	1.3	90.0	1.3	1.3	1.3	1.3
Sparse vegetation	4.07	7.70	2.68	0.00	0.03	15.09	1.26	0.05	0.00
	13.2	25.0	8.7	0.0	0.1	48.9	4.1	0.2	0.0
Bare area	0.33	0.00	1.99	0.01	0.17	2.90	14.82	0.09	0.00
	1.6	0.0	9.8	0.0	0.8	14.3	72.9	0.5	0.0
Water	0.11	1.26	0.09	0.57	0.07	0.16	1.01	15.56	0.00
	0.6	6.7	0.5	3.0	0.4	0.8	5.3	82.6	0.0
P. snow and Ice	0.00	0.00	0.00	0.00	1.68	0.00	0.00	0.00	15.10
	0.0	0.0	0.0	0.0	10.0	0.0	0.0	0.0	90.0

sparse vegetation and grassland, respectively. However, stability of bare area will decrease to 56% in 2050 with conversion of 17.9% and 15.4% to shrubland/sparse vegetation and grassland, respectively.

Although settlement (90%) and snow and ice (90%) are the most persistent classes in both 2030 and 2050, the predictions yet estimate a conversion of 1.3% from settlement to all other classes, and a conversion of 10% from snow and ice to settlement. Water is another persistent class (82.6% in 2030 and 73.9% in 2050) with only 6.7% (7.3%) and 5.3% (7.1%) conversion to forest and bare area in 2030 (2050), respectively. It is predicted that shrubland/sparse vegetation is another extremely vulnerable class characterized by 51.4% and 71.9% loss of its extent in 2030 and 2050, respectively, largely in favour of forest (25% in 2030 and 26.1% in 2050), agriculture (13.2% in 2030 and 23.2% in 2050) and grassland (8.7% in 2030 and 13.1% in 2050).

5. Discussions

This study investigated global landscape changes within 1992–2015 using ESA-CCI-LC dataset. Moreover, the study used predictive modelling for estimating the future landscape changes by 2030 and 2050. The analysis of historical changes reveals relatively massive dynamism across the planet and among different land types with minimum persistence in forest, agriculture and shrubland/sparse vegetation.

Although agriculture shows an increasing trend, a closer look at gain and loss analysis reveals that the class is highly dynamic, in which more than 1.3 million sqkm of agricultural lands were converted to other land types, while about 2.2 million sqkm went under cultivation. A loss of 1.3 million sqkm indicates lands abandoned in different regions (in particular Eastern Europe, Central African countries, South America and China) due to water shortage and other natural and anthropogenic causes. Agriculture class shows the maximum conversion rate from/to forest in all time periods. The conversions from agriculture to forest often lead to afforestation. On the other hand, when cultivable lands are abandoned, vegetation recovers into shrub, tall herb or even forest cover, depending on climatic and soil conditions. While there is no doubt that the two classes are closely related and converting to each other over time (often forest to agriculture), given the significant conversion rates, it is worth noting that a part of this conversion should be considered as the misclassification error of the two classes. This is because of the spectral similarities of agriculture and forest and the difficulty in separating them in the classification process. Given the fact that deforestation and land conversion for agriculture is an increasing threat to biodiversity conservation and climate change, massive conversion currently happening in the Amazon rainforest and Central-East Africa (see Fig. 5) and the predications of more than 30% by 2030 and 2050, is overwhelming and must be given a sharp focus. Although the

Table 3

The transition area matrix presenting the expected land change from the horizontal classes to the vertical classes in terms of million sqkm and percentage (2015–2050).

	Agriculture	Forest	Grassland	Wetland	Settlement	Sparse vegetation	Bare area	Water	P. snow and Ice
Agriculture	14.14	10.79	2.07	0.27	6.04	2.14	0.26	0.50	0.00
	39.0	29.8	5.7	0.7	16.7	5.9	0.7	1.4	0.0
Forest	12.42	9.88	3.84	1.77	1.28	6.58	0.63	1.30	0.00
	32.9	26.2	10.2	4.7	3.4	17.4	1.7	3.5	0.0
Grassland	4.33	3.53	11.46	0.09	0.95	3.13	1.02	0.19	0.00
	17.5	14.3	46.4	0.4	3.8	12.7	4.1	0.8	0.0
Wetland	0.86	4.93	0.26	10.23	0.05	0.59	0.02	0.30	0.00
	5.0	28.6	1.5	59.4	0.3	3.4	0.1	1.7	0.0
Settlement	0.11	0.11	0.11	0.11	8.13	0.11	0.11	0.11	0.11
	1.3	1.3	1.3	1.3	90.0	1.3	1.3	1.3	1.3
Sparse vegetation	6.44	7.25	3.64	0.24	0.55	7.81	1.57	0.29	0.00
	23.2	26.1	13.1	0.8	2.0	28.1	5.7	1.1	0.0
Bare area	0.91	0.54	2.82	0.00	0.35	3.27	10.25	0.15	0.00
	5.0	3.0	15.4	0.0	1.9	17.9	56.0	0.8	0.0
Water	0.45	1.24	0.26	0.72	0.11	0.44	1.20	12.52	0.00
	2.7	7.3	1.5	4.3	0.6	2.6	7.1	73.9	0.0
P. snow and Ice	0.00	0.00	0.00	0.00	1.51	0.00	0.00	0.00	13.59
	0.0	0.0	0.0	0.0	10.0	0.0	0.0	0.0	90.0

patterns in Fig. 5 may seem random, it is indeed the reflection of worldwide change/conversion among different LC classes as captured by such high spatial resolution dataset at global scale. This indicates the spread of change/conversion all over the planet appearing like speckle pixels.

It should be noted that derived agriculture statistics in the current study (an increase of about 0.8 million sqkm from 1992 to 2015) are not in accordance with Food and Agriculture Organization (FAO) agriculture inventory that was steady to some extent over the same period with little fluctuation from 48.614 million sqkm to 48.620 million sqkm. Likewise, FAO forest inventory shows a steady decline from 41.137 million sqkm in 1992 to 39.991 million sqkm in 2015 resulted in a remarkable deforestation of about 1.146 million sqkm over the time period of 24 years, while our findings show an overall decrease of about 0.357 million sqkm. These results could be partly explained by the fact that FAO and ESA-CCI-LC datasets significantly differ in their LC nomenclature, as well as they employ different methodologies and data sources. This, in turn, reveals the discrepancy between global LC datasets and poses this question: which dataset should be used as the reference for a particular purpose?

Consistent with the literature, this research found that dramatic settlement area expansion has been accompanied by loss of agriculture and grassland over the 24-year time period and will continue to consume more agriculture in the near future. It is clear that conversion from settlement to other LC types is very unlikely, hence, conversion rate of 1.3% to other classes can be considered as misclassification error. Similarly, 10% conversion from snow and ice to settlement is likely due to misclassification, given the fact that most permanent snow and ice covers are either located in high-elevation or subarctic and arctic regions, not suitable for urban expansion. These results further support the idea of vast agriculture conversion to settlement in 2030 and 2050. Loss of agriculture along with rapid increase of population and hence human settlement is going to become a serious global challenge threatening food security in future. Our findings indicate that forest and shrubland/sparse vegetation were the most vulnerable classes from 1992 to 2015 and continue to be extremely vulnerable in 2030 and 2050 with overall stability of less than 40%. Agriculture and grassland will be also very vulnerable classes in 2050 with less than 50% stability.

Converting about 5.3% of water to bare land is likely implying disappearing inland water bodies e.g., lakes, streams, rivers as reported recently such as Urmia lake and Bakhtegan lake (Iran), Aral Sea (Kazakhstan and Uzbekistan), and Lake Chad. Conversion from settlement to other cover type are not likely to happen and this is due to data accuracy. A constant value of transition from settlement to other class types is likely due to uncertainty in the classified LC. Conversion from wetland to forest (24.5% for 2030 and 28.6% for 2050) could be partly due to misclassification and partly due to drying out wetland and being replaced by some vegetation cover e.g., Canada, Brazil, Paraguay, and Bolivia. Conversion of 10% from snow and ice to settlement could not be explained, as this conversion is not likely to happen.

The major concern arises when these changes occurred only within 24 years and if the same rate of change is to come, overwhelming landscape changes must be expected. In terms of the predictive analysis used in this study, a simple and straightforward model was utilized, therefore, future studies should look into more advanced models with respect to considering relevant environmental, physical, and socio-economic factors. Furthermore, it is recommended to investigate the outputs from different modelling techniques and explore to what degree the results can vary through uncertainty analysis. Due to the size and global extent of this study, this task has to be carried out in another study.

With respect to the comprehensiveness of ESA-CCI-LC nomenclature, it is one of the richest nomenclatures compared to other global datasets by covering 37 land types. This offers a big advantage for end-users by having a wide variety of land types and the possibility of

merging them for a specific application. Moreover, it offers the flexibility to distinct between sub-classes of a land type, for instance, subclasses of forest, agriculture, shrubland.

Finally, our findings/discussions might be useful to a wide range of stakeholders, academics, land managers, and environmentalists for a) what kind of changes are occurring across the planet and how they might affect our environment with respect to anthropogenic intervention, public health, socio-economic changes, b) how effective our local, regional, and global environmental and land policies are and whether they are environment-friendly or destructive so that necessary precautions could be dispatched, c) what advantages and disadvantages ESA-CCI-LC dataset present, d) what extreme land processes e.g., deforestation, urbanization, water shrinkage are taking place at country and continent level, and e) how ESA-CCI-LC dataset can contribute to achieving the united nations (UN) sustainable goals and what feedback can be given to the data providers with respect to these goals.

6. Conclusions

ESA-CCI-LC dataset is the first global LC map with comparatively better spatial and temporal coverage, which can answer to a number of research questions that require such a dataset for yearly observations. A wide range of applications can be built based on this dataset. To name a few, estimation of food production, CO₂ emission, population density, ice and snow fluctuations, desertification, afforestation/deforestation, poverty, and compliance with the Paris UNFCCC Agreement can be named. It would be interesting to conduct cross dataset comparisons and check the source of discrepancy among different products. Additionally, the use of citizen observatories in improving the quality of this dataset is worthwhile investigating. Instances such as [Geo-Wiki.org](https://www.geo-wiki.org/) (Fritz et al., 2012) and [openstreetmap.org](https://www.openstreetmap.org/) (J. Jokar Arsanjani, Mooney, Zipf, & Schauss, 2015) can be mentioned.

While a few studies have looked into the land change process in developing countries, it is important to conduct studies exploring the underlying changes and communicate the outcomes with the respective local/regional/global authorities. Although Markov transition matrices are not spatial output indicating where the changes will happen, they are definitely useful in terms of estimating the future changes alarming policy makers about future planning. For instance, if the current change trend is about to continue, main cover types including forest, shrubland/sparse vegetation, agriculture and wetland will become less stable meaning of losing more lands to other types such as bare land and settlements. The most striking conversion rate is from forest to agriculture (2030) with 7 million hectare per month (more than 90 times the area of New York City). Conversion of forest (30%) cover to agriculture and similarly 19% to shrubland is like a ticking bomb for the environment and global climate change.

It should be noted that the presented statistics can vary from one global LC dataset to another. In other words, there might be a large discrepancy between statistical numbers from this dataset and FAO for class forest as mentioned in Section 4. This is of course dependent on a) the scope and objective of producing it i.e., whether it is for agricultural monitoring or climate change studies, etc. b) the process and methodology of data production, c) the achieved data quality and the data quality assessment mechanism, and d) the projection system used while reporting statistics.

Our study reports the global changes and we believe local land change modelling can give a better and more precise picture of local land processes. Hence, this study should foster the interest of looking at dynamic areas and explore them more accurately. One of the drawbacks of this dataset is that it does not distinct inland water from open waters. It is important to have these classes separately as we are witnessing the shrinkage of lakes and inland water bodies. Furthermore, small water bodies and rivers are not well mapped due to the spatial resolution of the dataset at 300 m. Water-related studies should take this drawback into consideration and use ancillary datasets for that purpose. These

predictions shed light into the situation of different LC types in the near future and raise a big alarm towards protecting forest, agriculture, shrubland/sparse vegetation and grassland to be converted to other LC types.

Finally, as we are facing big global problems e.g., climate change, big geographical data including remote sensing data and open data are becoming unprecedentedly available and, hence, we should exploit big earth data for addressing major challenges.

Appendix A. Supplementary data

Supplementary data to this article can be found online at <https://doi.org/10.1016/j.apgeog.2019.03.010>.

References

- Aburas, M. M., Ho, Y. M., Ramli, M. F., & Ashaari, Z. H. (2016). The simulation and prediction of spatio-temporal urban growth trends using cellular automata models: A review. *International Journal of Applied Earth Observation and Geoinformation*, 52, 380–389. <https://doi.org/10.1016/j.jag.2016.07.007>.
- Alimohammadi, A., Mousivand, A., & Shayan, S. (2010). Prediction of land use and land cover changes by using multi-temporal satellite imagery and Markov chain model. *Spatial Planning*, 14(367) 17–130.
- Alo, C. A., & Robert Gilmore Pontius, J. (2008). Identifying systematic land-cover transitions using remote sensing and GIS: The fate of forests inside and outside protected areas of Southwestern Ghana. *Environment and Planning B: Planning and Design*, 35(2), 280–295. <https://doi.org/10.1068/b32091>.
- Arino, O., Ramos Perez, J. J., Kalogirou, V., Bontemps, S., Defourny, P., & Van Bogaert, E. (2012). *Global land cover map for 2009 (GlobCover 2009)*. PANGAEA <https://doi.org/10.1594/PANGAEA.787668>.
- Arsanjani, J. J. (2018). Characterizing, monitoring, and simulating land cover dynamics using Globeland30: A case study from 2000 to 2030. *Journal of Environmental Management*, 214, 66–75.
- Bartholomé, E., & Belward, A. S. (2005). GLC2000: A new approach to global land cover mapping from earth observation data. *International Journal of Remote Sensing*, 26(9), 1959–1977. <https://doi.org/10.1080/01431160412331291297>.
- Bojinski, S., Verstraete, M., Peterson, T. C., Richter, C., Simmons, A., & Zemp, M. (2014). The concept of essential climate Variables in support of climate research, applications, and policy. *Bulletin of the American Meteorological Society*, 95, 1431–1443.
- Clarke, K. C., & Gaydos, L. J. (1998). Loose-coupling a cellular automaton model and GIS: Long-term urban growth prediction for San Francisco and Washington/Baltimore. *International Journal of Geographical Information Science*, 12(7), 699–714. <https://doi.org/10.1080/136588198241617>.
- Defourny, P., Moreau, I., & Bontemps, S. (2017). *P roduct U ser G uide*.
- Defourny, P., Schouten, L., Bartalev, S., Bontemps, S., Caccetta, P., De Wit, A. J. W., et al. (2008). Accuracy assessment of a 300 m global land cover map: The GlobCover experience.
- Deus, D., & Gloaguen, R. (2013). Remote sensing analysis of lake dynamics in semi-arid regions: Implication for water resource management. Lake Manyara, East African Rift, Northern Tanzania. *Water*, 5(2), 698–727. <https://doi.org/10.3390/w5020698>.
- Dubovoyk, O., Sliuzas, R., & Flacke, J. (2011). Spatio-temporal modelling of informal settlement development in Sancaktepe district, Istanbul, Turkey. *ISPRS Journal of Photogrammetry and Remote Sensing*, 66(2), 235–246. <https://doi.org/10.1016/j.isprsjprs.2010.10.002>.
- Ellis, E. C., & Ramankutty, N. (2008). Putting people in the map: Anthropogenic biomes of the world. *Frontiers in Ecology and the Environment*, 6(8), 439–447.
- Feddema, J. J., Oleson, K. W., Bonan, G. B., Mearns, L. O., Buja, L. E., Meehl, G. A., et al. (2005). The importance of land-cover change in simulating future climates. *Science*, 310(5754), 1674. <https://doi.org/10.1126/science.1118160>.
- Foley, J. A., DeFries, R., Asner, G. P., Barford, C., Bonan, G., Carpenter, S. R., et al. (2005). Global consequences of land use. *Science*, 309(5734), 570–574.
- Friedl, M. A., McIver, D. K., Hodges, J. C. F., Zhang, X. Y., Muchoney, D., Strahler, A. H., et al. (2002). Global land cover mapping from MODIS: Algorithms and early results. *Remote Sensing of Environment*, 83(1), 287–302.
- Fritz, S., McCallum, I., Schill, C., Perger, C., See, L., Schepaschenko, D., et al. (2012). Geo-Wiki: An online platform for improving global land cover. *Environmental Modelling & Software*, 31(0), 110–123. <https://doi.org/10.1016/j.envsoft.2011.11.015>.
- Fuchs, R., Prestele, R., & Verburg, P. H. (2018). A global assessment of gross and net land change dynamics for current conditions and future scenarios. *Earth System Dynamics*, 9(2), 441–458. <https://doi.org/10.5194/esd-9-441-2018>.
- Grekousis, G., Mountrakis, G., & Kavouras, M. (2015). An overview of 21 global and 43 regional land-cover mapping products. *International Journal of Remote Sensing*, (January), 1–27. <https://doi.org/10.1080/01431161.2015.1093195>.
- Haase, D., Lautenbach, S., & Seppelt, R. (2010). Modeling and simulating residential mobility in a shrinking city using an agent-based approach. *Environmental Modelling & Software*, 25(10), 1225–1240. <https://doi.org/10.1016/j.envsoft.2010.04.009>.
- Hansen, M. C., DeFries, R. S., Townshend, J. R. G., & Sohlberg, R. (2000). Global land cover classification at 1 km spatial resolution using a classification tree approach. *International Journal of Remote Sensing*, 21(6–7), 1331–1364.
- Higginbottom, T. P., & Symeonakis, E. (2014). Assessing land degradation and desertification using vegetation index data: Current frameworks and future directions. *Remote Sensing*, 6(10), 9552–9575.
- Janetos, A. C., Lambin, E. F., Lepers, E., Achard, F., Ramankutty, N., Scholes, R. J., et al. (2005). A synthesis of information on rapid land-cover change for the period 1981–2000. *BioScience*, 55(2), 115–124. [https://doi.org/10.1641/0006-3568\(2005\)055\[0115:ASOIOR\]2.0.CO;2](https://doi.org/10.1641/0006-3568(2005)055[0115:ASOIOR]2.0.CO;2).
- Janssen, S., Dumont, G., Fierens, F., & Mensink, C. (2008). Spatial interpolation of air pollution measurements using CORINE land cover data. *Atmospheric Environment*, 42(20), 4884–4903.
- Jokar Arsanjani, J., Fibæk, C. S., & Vaz, E. (2018). Development of a cellular automata model using open source technologies for monitoring urbanisation in the global south: The case of Maputo, Mozambique. *Habitat International*, 71, 38–48. <https://doi.org/https://doi.org/10.1016/j.habitatint.2017.11.003>.
- Jokar Arsanjani, J., Helbich, M., & Vaz, E. (2013). Spatiotemporal simulation of urban growth patterns using agent-based modeling: The case of Tehran. *Cities*, 32, 33–42. <https://doi.org/https://doi.org/10.1016/j.cities.2013.01.005>.
- Jokar Arsanjani, T., Javidan, R., Nazemosadat, M. J., Jokar Arsanjani, J., & Vaz, E. (2015b). Spatiotemporal monitoring of Bakhtegan Lake's areal fluctuations and an exploration of its future status by applying a cellular automata model. *Computers & Geosciences*, 78(0), 37–43. <https://doi.org/https://doi.org/10.1016/j.cageo.2015.02.004>.
- Jokar Arsanjani, J., Kainz, W., & Mousivand, A. J. (2011). Tracking dynamic land-use change using spatially explicit Markov chain based on cellular automata: The case of Tehran. *International Journal of Image and Data Fusion*, 2(4), 329–345. <https://doi.org/10.1080/19479832.2011.605397>.
- Jokar Arsanjani, J., Mooney, P., Zipf, A., & Schauss, A. (2015a). Quality assessment of the contributed land use information from OpenStreetMap versus authoritative datasets. *Lecture notes in geoinformation and cartography* https://doi.org/10.1007/978-3-319-14280-7_3.
- Kamusoko, C., Aniya, M., Adi, B., & Manjoro, M. (2009). Rural sustainability under threat in Zimbabwe – Simulation of future land use/cover changes in the Bindura district based on the Markov-cellular automata model. *Applied Geography*, 29(3), 435–447. <https://doi.org/10.1016/j.apgeog.2008.10.002>.
- Lambin, E. F., Turner, B. L., Geist, H. J., Agbola, S. B., Angelsen, A., Bruce, J. W., et al. (2001). The causes of land-use and land-cover change: Moving beyond the myths. *Global Environmental Change*, 11(4), 261–269. [https://doi.org/10.1016/S0959-3780\(01\)00007-3](https://doi.org/10.1016/S0959-3780(01)00007-3).
- Li, W., Ciaia, P., MacBean, N., Peng, S., Defourny, P., & Bontemps, S. (2016). Major forest changes and land cover transitions based on plant functional types derived from the ESA CCI Land Cover product. *International Journal of Applied Earth Observation and Geoinformation*, 47, 30–39. <https://doi.org/10.1016/j.jag.2015.12.006>.
- Li, W., Macbean, N., Ciaia, P., Defourny, P., Lamarche, C., Bontemps, S., et al. (2018). Gross and net land cover changes in the main plant functional types derived from the annual ESA CCI land cover maps (1992–2015). *Earth System Science Data*, 10(1), 219–234. <https://doi.org/10.5194/essd-10-219-2018>.
- Liu, X., Yu, L., Li, W., Peng, D., Zhong, L., Li, L., et al. (2018a). Comparison of country-level cropland areas between ESA-CCI land cover maps and FAOSTAT data. *International Journal of Remote Sensing*, 1161, 1–15. <https://doi.org/10.1080/01431161.2018.1465613>.
- Liu, X., Yu, L., Si, Y., Zhang, C., Lu, H., Yu, C., et al. (2018b). Identifying patterns and hotspots of global land cover transitions using the ESA CCI Land Cover dataset. *Remote Sensing Letters*, 9(10), 972–981. <https://doi.org/10.1080/2150704X.2018.1500070>.
- Loveland, T. R., Reed, B. C., Brown, J. F., Ohlen, D. O., Zhu, Z., Yang, L., et al. (2000). Development of a global land cover characteristics database and IGBP DISCover from 1 km AVHRR data. *International Journal of Remote Sensing*, 21(6–7), 1303–1330. <https://doi.org/10.1080/014311600210191>.
- Mahmood, R., Pielke, R. A., & McAlpine, C. A. (2015). Climate-relevant land use and land cover change policies. *Bulletin of the American Meteorological Society*, 97(2), 195–202. <https://doi.org/10.1175/BAMS-D-14-00221.1>.
- Nunes, J., Loures, L., Lopez-Piñeiro, A., Loures, A., & Vaz, E. (2016). Using GIS towards the characterization and soil mapping of the caia irrigation perimeter. *Sustainability*, 8(4), 368. <https://doi.org/10.3390/su8040368>.
- Pineda Jaimes, N. B., Bosque Sendra, J., Gómez Delgado, M., & Franco Plata, R. (2010). Exploring the driving forces behind deforestation in the state of Mexico (Mexico) using geographically weighted regression. *Applied Geography*, 30(4), 576–591. <https://doi.org/10.1016/j.apgeog.2010.05.004>.
- Plummer, S., Lecomte, P., & Doherty, M. (2017). The ESA climate change initiative (CCI): A European contribution to the generation of the global climate observing system. *Remote Sensing of Environment*, 203, 2–8. <https://doi.org/10.1016/j.rse.2017.07.014>.
- Rindfuss, R. R., Walsh, S. J., Turner, B. L., Fox, J., & Mishra, V. (2004). Developing a science of land change: Challenges and methodological issues. *Proceedings of the National Academy of Sciences of the United States of America*, 101(39), 13976 LP-13981 <https://doi.org/10.1073/pnas.0401545101>.
- Roach, J. K., Griffith, B., & Verbyla, D. (2013). Landscape influences on climate-related lake shrinkage at high latitudes. *Global Change Biology*, 19, 2276–2284. <https://doi.org/10.1111/gcb.12196>.
- Seto, K. C., Güneralp, B., & Hutyra, L. R. (2012). Global forecasts of urban expansion to 2030 and direct impacts on biodiversity and carbon pools. *Proceedings of the National Academy of Sciences of the United States of America*, 109(40), 16083–16088. <https://doi.org/10.1073/pnas.1211658109>.
- Sternberg, T., Tsolmon, R., Middleton, N., & Thomas, D. (2011). Tracking desertification on the Mongolian steppe through NDVI and field-survey data. *International Journal of Digital Earth*, 4(1), 50–64.
- Symeonakis, E. (2016). Modelling land cover change in a Mediterranean environment using Random Forests and a multi-layer neural network model. *Geoscience and remote sensing symposium (IGARSS), 2016 IEEE international* (pp. 5464–5466). IEEE.

- Tayyebi, A., & Pijanowski, B. C. (2014). Modeling multiple land use changes using ANN, CART and MARS: Comparing tradeoffs in goodness of fit and explanatory power of data mining tools. *International Journal of Applied Earth Observation and Geoinformation*, 28(0), 102–116. <https://doi.org/https://doi.org/10.1016/j.jag.2013.11.008>.
- Turner, B. L., Lambin, E. F., & Reenberg, A. (2007). The emergence of land change science for global environmental change and sustainability. *Proceedings of the National Academy of Sciences*, 104(52), 20666–20671.
- Vaz, E., & Arsanjani, J. J. (2015). Predicting urban growth of the greater toronto area - coupling a markov cellular automata with document meta-analysis. *Journal of Environmental Informatics*, 25(2)<https://doi.org/10.3808/jei.201500299>.
- Verburg, P. H., Eck, J. R. R. Van, Nijs, T. C. M. De, Dijst, M. J., & Schot, P. (2004). Determinants of land-use change patterns in The Netherlands. *Environment and Planning B: Planning and Design*, 31(1), 125–150. <https://doi.org/10.1068/b307>.
- Verburg, P. H., Neumann, K., & Nol, L. (2011). Challenges in using land use and land cover data for global change studies. *Global Change Biology*, 17(2), 974–989. <https://doi.org/10.1111/j.1365-2486.2010.02307.x>.
- Verburg, P. H., & Overmars, K. P. (2009). Combining top-down and bottom-up dynamics in land use modeling: Exploring the future of abandoned farmlands in Europe with the Dyna-CLUE model. *Landscape Ecology*, 24(9), 1167. <https://doi.org/10.1007/s10980-009-9355-7>.
- Wulder, M. A., White, J. C., Goward, S. N., Masek, J. G., Irons, J. R., Herold, M., et al. (2008). Landsat continuity: Issues and opportunities for land cover monitoring. *Remote Sensing of Environment*, 112(3), 955–969.
- Yang, X., Zheng, X.-Q., & Chen, R. (2014). A land use change model: Integrating landscape pattern indexes and Markov-CA. *Ecological Modelling*, 283, 1–7. <https://doi.org/10.1016/j.ecolmodel.2014.03.011>.
- Zhang, T., Liu, G., Zhu, Z., Gong, W., Ji, Y., & Huang, Y. (2016). Real-time estimation of satellite-derived PM2.5 based on a semi-physical geographically weighted regression model. *International Journal of Environmental Research and Public Health*. <https://doi.org/10.3390/ijerph13100974>.
- Zhou, D., Lin, Z., & Liu, L. (2012). Regional land salinization assessment and simulation through cellular automaton-Markov modeling and spatial pattern analysis. *Science of The Total Environment*, 439, 260–274. <https://doi.org/10.1016/j.scitotenv.2012.09.013>.